Journal of Applied Mathematics & Bioinformatics, vol.1, no.1, 2011, 31-54
ISSN: 1792-6602 (print), 1792-6939 (online)

MHD Couette flow of class-II in a rotating system

G. S. Seth[1], S. M. Hussain[2] and J. K. Singh[3]

Abstract

Steady MHD Couette flow of class-II of a viscous incompressible electrically conducting fluid in a rotating system is studied. Exact solution of the governing equations is obtained in closed form. Expressions for the shear stress at lower and upper plates due to primary and secondary flows and mass flow rates in primary and secondary flow directions are derived. Asymptotic behavior of the solution for velocity and induced magnetic field is analyzed for small and large values of rotation parameter K^2 and magnetic parameter M^2 to gain some physical insight into flow pattern. Heat transfer characteristics of the fluid are considered taking viscous and Joule dissipations into account. Numerical solution of energy equation and numerical values of rate of heat transfer at lower and upper plates are computed with the help of MATLAB software. The numerical values of velocity, induced magnetic field and fluid temperature are displayed graphically versus channel width variable η for various values of pertinent flow parameters whereas numerical values of the shear stress at lower and upper plates due to

---

[1] Department of Applied Mathematics, Indian School of Mines, Dhanbad-826004, India, e-mail: gsseth_ism@yahoo.com.
[2] Department of Mathematics, O. P. Jindal Institute of Technology, Punjipathra, Raigarh-496001, India, e-mail: hussain.modassir@yahoo.com.
[3] Department of Applied Mathematics, Indian School of Mines, Dhanbad-826004, India, e-mail: s.jitendrak@yahoo.com.

Article Info: *Revised* : February 15, 2011. *Published online* : May 31, 2011.

primary and secondary flows, mass flow rates in primary and secondary flow directions and rate of heat transfer at lower and upper plates are presented in tabular form for various values of pertinent flow parameters.

Mathematics Subject Classification: 76U05: Rotating Fluids

Keywords: Magnetic field, Coriolis force, modified Ekman boundary layer, Hartmann boundary layer, viscous and Joule dissipations.

1 Introduction

Investigation of hydromagnetic flows with or without heat transfer assumes significance due to occurrence of such type of fluid flows in numerous areas of engineering and applied physics. A prominent area of focus is MHD energy generator flows which include disk systems [1], solar pond hydromagnetic generators [2] and magneto-thermo-acoustic generators [3]. Other areas of application are hypersonic ionized boundary layers [4], particle deposition in electrically-conducting systems [5] and liquid metal processing [6]. In numerous MHD flows rotation may also take place and Coriolis and centrifugal forces can exert a significant effect on fluid flows and heat transfer processes. Keeping in view this fact Jana et al. [7], Jana and Datta [8], Seth and Maiti [9], Mandal et al. [10], Mandal and Mandal [11], Seth and Ahmad [12], Kumar et al. [13], Seth et al. [14-19], Chandran et al. [20], Singh et al. [21], Singh [22], Hayat et al. [23, 24] and Guria et al. [25] investigated MHD Couette flow of a viscous incompressible electrically conducting fluid in a rotating system considering different aspects of the problem.

It is worthy to note that there may be two types of MHD Couette flow viz. (i) MHD Couette flow of class-I and (ii) MHD Couette flow of class-II. The fluid flow induced due to movement of a plate, when fluid is bounded by a stationary plate placed at a finite distance from the moving plate, may be recognized as

MHD Couette flow of class-I. This fluid flow is similar to the flow induced due to movement of a plate when the free stream is stationary. The fluid flow past a stationary plate, which is induced due to movement of a plate placed at a finite distance from the stationary plate, may be recognized as MHD Couette flow of class-II. This fluid flow is similar to the fluid flow past a stationary plate due to moving free stream. Research studies carried out by Jana et al. [7], Jana and Datta [8], Seth and Maiti [9], Mandal et al. [10], Mandal and Mandal [11], Seth and Ahmad [12], Kumar et al. [13], Seth et al. [14-18], Chandran et al. [20], Singh et al. [21] and Guria et al. [25] belong to MHD Couette flow of class-I. Seth et al. [19], Singh [22] and Hayat et al. [23, 24] investigated MHD Couette flow of class-II in a rotating system in the presence of a uniform transverse magnetic field considering different aspects of the problem. In their studies the induced magnetic field produced by fluid motion is negligible in comparison to the applied one. It is well known that the induced magnetic field produced by fluid motion is negligible in comparison to applied one when magnetic Reynolds number is very small. However, for the problems of astrophysical and geophysical interest magnetic Reynolds number is not very small. For such type of fluid flow problems induced magnetic field plays a significant role in determining flow features of the problem.

The purpose of the present investigation is to study steady MHD Couette flow of class-II of a viscous incompressible electrically conducting fluid in a rotating system in the presence of a uniform transverse magnetic field applied parallel to the axis of rotation by taking induced magnetic field into account.

2 Formulation of the Problem and Its Solution

Consider a steady flow of a viscous incompressible electrically conducting fluid between two parallel plates $z=0$ and $z=L$ in the presence of a uniform transverse magnetic field H_0 applied parallel to z axis. The lower plate is perfectly conducting whereas upper plate is non-conducting. Both the fluid and channel are in a state of rigid body rotation with uniform angular velocity Ω

about z-axis. Flow within the channel is induced due to movement of the upper plate $z = L$ with a uniform velocity U_0 in x-direction while lower plate $z = 0$ is kept fixed. Since plates of the channel are of infinite extent in x and y-directions and fluid flow is steady so all physical quantities, except pressure, depend on z only. Therefore, fluid velocity $\vec{q}$ and induced magnetic field $\vec{H}$ are given by

$$\vec{q} = (u^*, v^*, 0) \text{ and } \vec{H} = (H_x^*, H_y^*, H_0)\,. \tag{1}$$

This assumption is in agreement with the fundamental equations of Magnetohydrodynamics in a rotating frame of reference.

Taking into consideration of the assumption made above, the governing equations for fluid flow of a viscous incompressible electrically conducting fluid in a rotating frame of reference are

$$-2\Omega v^* = -\frac{1}{\rho}\frac{\partial p^*}{\partial x} + \upsilon \frac{d^2 u^*}{dz^2} + \frac{\mu_e H_0}{\rho}\frac{dH_x^*}{dz}, \tag{2}$$

$$2\Omega u^* = -\frac{1}{\rho}\frac{\partial p^*}{\partial y} + \upsilon \frac{d^2 v^*}{dz^2} + \frac{\mu_e H_0}{\rho}\frac{dH_y^*}{dz}, \tag{3}$$

$$0 = -\frac{1}{\rho}\frac{\partial p^*}{\partial z}, \tag{4}$$

$$0 = H_0 \frac{du^*}{dz} + \eta_m \frac{d^2 H_x^*}{dz^2}, \tag{5}$$

$$0 = H_0 \frac{dv^*}{dz} + \eta_m \frac{d^2 H_y^*}{dz^2}, \tag{6}$$

where $\eta_m = 1/\mu_e \sigma$ and ρ, υ, μ_e, σ and p^* are, respectively, fluid density, kinematic coefficient of viscosity, magnetic permeability, electrical conductivity of the fluid and modified pressure including centrifugal force.

The boundary conditions for the velocity and induced magnetic field are

$$u^* = v^* = 0 \quad \text{at } z = 0, \tag{7a}$$

$$u^* = U_0,\ v^* = 0 \quad \text{at } z = L, \tag{7b}$$

$$\frac{dH_x^*}{dz} = \frac{dH_y^*}{dz} = 0 \quad \text{at} \quad z = 0, \tag{8a}$$

$$H_x^* = H_y^* = 0 \qquad \text{at} \quad z = L. \tag{8b}$$

Equation (4) shows constancy of modified pressure p^* along z-axis i.e. axis of rotation. It may be noted that a number of investigations on MHD Couette flow are carried out in the past. Keeping in view the research studies made on MHD Couette flow till now, we are the opinion that MHD Couette flow may be classified in two forms, namely, (i) MHD Couette flow of class-I and (ii) MHD Couette flow of class-II. The fluid flow induced due to movement of a plate, when fluid is bounded by a stationary plate placed at a finite distance from the moving plate, may be recognized as MHD Couette flow of class-I. This fluid flow is similar to the flow induced due to movement of a plate when the free stream is stationary. The fluid flow past a stationary plate, which is induced due to movement of a plate placed at a finite distance from the stationary plate, may be recognized as MHD Couette flow of class-II. This fluid flow is similar to the fluid flow past a stationary plate due to moving free stream. For MHD Couette flow of class-I the pressure gradient terms $-\frac{1}{\rho}\frac{\partial p^*}{\partial x}$ and $-\frac{1}{\rho}\frac{\partial p^*}{\partial y}$, which are present in equations (2) and (3) respectively, are not considered by researchers [7-18, 20, 21, 25]. This assumption is justified and it is clearly evident from conditions (7a) and (8a). For MHD Couette flow of class-II values of the pressure gradient terms in equations (2) and (3) are evaluated with the help of boundary conditions (7b) and (8b) which are given by

$$-\frac{1}{\rho}\frac{\partial p^*}{\partial x} = 0 \quad \text{and} \quad -\frac{1}{\rho}\frac{\partial p^*}{\partial y} = 2\Omega U_0. \tag{9}$$

Equations (2) and (3) with the use of (9) become

$$-2\Omega v^* = \upsilon\frac{d^2u^*}{dz^2} + \frac{\mu_e H_0}{\rho}\frac{dH_x^*}{dz}, \tag{10}$$

$$2\Omega(u^* - U_0) = \upsilon \frac{d^2 v^*}{dz^2} + \frac{\mu_e H_0}{\rho} \frac{dH_y{}^*}{dz}. \tag{11}$$

Representing equations (10), (11), (5) and (6), in non-dimensional form, we obtain

$$-2K^2 v = \frac{d^2 u}{d\eta^2} + \frac{M^2}{R_m} \frac{dH_x}{d\eta}, \tag{12}$$

$$2K^2(u-1) = \frac{d^2 v}{d\eta^2} + \frac{M^2}{R_m} \frac{dH_y}{d\eta}, \tag{13}$$

$$0 = \frac{du}{d\eta} + \frac{1}{R_m} \frac{d^2 H_x}{d\eta^2}, \tag{14}$$

$$0 = \frac{dv}{d\eta} + \frac{1}{R_m} \frac{d^2 H_y}{d\eta^2}, \tag{15}$$

where

$$\left.\begin{aligned} &\eta = z/L, u = u^*/U_0, v = v^*/U_0, H_x = H_x{}^*/H_0, H_y = H_y{}^*/H_0, \\ &K^2 = \Omega L^2/\upsilon, M^2 = \mu_e{}^2 H_0{}^2 L^2(\sigma/\rho\upsilon), R_m = U_0 L/\eta_m. \end{aligned}\right\} \tag{16}$$

Here K^2 is rotation parameter which is reciprocal of Ekman number, M^2 is magnetic parameter which is square of Hartmann number and R_m is magnetic Reynolds number.

The boundary conditions (7a) to (8b), in non-dimensional form, become

$$u = v = 0 \quad \text{at } \eta = 0; \ u = 1, \ v = 0 \quad \text{at } \eta = 1, \tag{17}$$

$$\frac{dH_x}{d\eta} = \frac{dH_y}{d\eta} = 0 \quad \text{at } \eta = 0; \ H_x = H_y = 0 \ \text{ at } \eta = 1. \tag{18}$$

Equations (12) to (15) are presented in compact form as

$$2iK^2(f-1) = \frac{d^2 f}{d\eta^2} + M^2 \frac{db}{d\eta}, \tag{19}$$

$$0 = \frac{df}{d\eta} + \frac{d^2 b}{d\eta^2}, \tag{20}$$

where $f = u + iv$, $b = h_x + ih_y$, $h_x = H_x/R_m$ and $h_y = H_y/R_m$.

The boundary conditions (17) and (18), in compact form, become

$$f = 0 \text{ at } \eta = 0 \text{ and } f = 1 \text{ at } \eta = 1, \tag{21}$$

$$\frac{db}{d\eta} = 0 \text{ at } \eta = 0 \text{ and } b = 0 \text{ at } \eta = 1. \tag{22}$$

Equations (19) and (20) together with the boundary conditions (21) and (22) are solved and solution for the velocity field and induced magnetic field are expressed in the following form

$$f = \frac{1}{\lambda}\left[A\sinh(\lambda\eta) + B(\cosh(\lambda\eta) - 1)\right], \tag{23}$$

$$b = \frac{1}{\lambda^2}\left[A(\cosh\lambda - \cosh(\lambda\eta)) + B\left\{\sinh\lambda - \sinh(\lambda\eta) + \frac{2iK^2\lambda(1-\eta)}{M^2}\right\}\right] + \frac{2iK^2(1-\eta)}{M^2}, \tag{24}$$

where $\lambda = \alpha + i\beta;\quad \alpha, \beta = \frac{1}{\sqrt{2}}\left[\left\{M^4 + 4K^4\right\}^{1/2} \pm M^2\right]^{1/2},$ (25a)

$$A = \frac{1}{\lambda\sinh\lambda}\left[M^2 + 2iK^2\cosh\lambda\right];\quad B = -\frac{2iK^2}{\lambda}. \tag{25b}$$

Shear Stress at the plates

The non-dimensional shear stress components τ_x and τ_y at lower and upper plates, due to the primary and secondary flows respectively, are given by

$$\tau_x + i\tau_y\big|_{\eta=0} = A, \quad \tau_x + i\tau_y\big|_{\eta=1} = A\cosh\lambda + B\sinh\lambda. \tag{26}$$

Mass Flow Rates

The non-dimensional mass flow rates Q_x and Q_y, in the primary and secondary flow directions, are given by

$$Q_x + iQ_y = \frac{1}{\lambda^2}\left[A(\cosh\lambda - 1) + B(\sinh\lambda - \lambda)\right]. \tag{27}$$

3 Asymptotic Solutions

We shall now discuss asymptotic behavior of the solution given by (23) to (25) for small and large values of M^2 and K^2 to gain some physical insight into the flow pattern.

Case I: $M^2 \ll 1$ and $K^2 \ll 1$

Since M^2 and K^2 are very small, neglecting squares and higher powers of M^2 and K^2 and their product in equations (23) to (25), we obtain velocity and induced magnetic field as

$$u = \eta - \frac{M^2}{6}\eta(1-\eta^2) + \cdots, \tag{28}$$

$$v = \frac{K^2}{3}\eta(2-3\eta+\eta^2) + \cdots, \tag{29}$$

$$h_x = \frac{1}{2}(1-\eta^2) - \frac{M^2}{24}(1-2\eta^2+\eta^4) + \cdots, \tag{30}$$

$$h_y = \frac{K^2}{12}(1-4\eta^2+4\eta^3-\eta^4) + \cdots. \tag{31}$$

The expressions (28) to (31) reveal that in a slowly rotating system when the conductivity of the fluid is low and/or applied magnetic field is weak, primary velocity u and primary induced magnetic field h_x are independent of rotation while secondary velocity v and secondary induced magnetic field h_y are unaffected by applied magnetic field.

Case II: $K^2 \gg 1$ and $M^2 \sim O(1)$

When K^2 is large and M^2 is of small order of magnitude fluid flow becomes boundary layer type. For the boundary layer flow adjacent to the upper plate $\eta = 1$, we introduce boundary layer co-ordinate $\xi = 1-\eta$, and obtain velocity and induced magnetic field from equations (23) to (25) as

$$u = 1 - \frac{M^2}{2K^2} e^{-\alpha_1 \xi} \sin \beta_1 \xi \,, \tag{32}$$

$$v = \frac{M^2}{2K^2} \left[1 - e^{-\alpha_1 \xi} \cos \beta_1 \xi \right], \tag{33}$$

$$h_x = \xi + \frac{M^2}{4K^3} \left[e^{-\alpha_1 \xi} \left\{ \cos \beta_1 \xi + \sin \beta_1 \xi \right\} - 1 \right], \tag{34}$$

$$h_y = \frac{M^2 \xi}{2K^2} + \frac{M^2}{4K^3} \left[e^{-\alpha_1 \xi} \left\{ \cos \beta_1 \xi - \sin \beta_1 \xi \right\} - 1 \right], \tag{35}$$

where

$$\alpha_1 = K \left(1 + \frac{M^2}{4K^2} \right), \quad \beta_1 = K \left(1 - \frac{M^2}{4K^2} \right). \tag{36}$$

It is revealed from the expressions (32) to (36) that there arises a thin boundary layer of thickness $O(1/\alpha_1)$ adjacent to the moving plate of the channel. This boundary layer may be identified as modified Ekman boundary layer and can be viewed as Ekman boundary layer modified by magnetic field. The thickness of this boundary layer decreases with increase in either M^2 or K^2. Similar type of boundary layer arises near lower plate of the channel. Exponential terms in the expressions (32) to (35) damp out quickly as ξ increases. When $\xi > 1/\alpha_1$ i.e. outside the boundary layer region, we obtain

$$u \approx 1, \qquad v \approx \frac{M^2}{2K^2}, \tag{37}$$

$$h_x \approx \xi - \frac{M^2}{4K^3}, \; h_y \approx \frac{M^2}{2K^2} \left(\xi - \frac{1}{2K} \right). \tag{38}$$

It is evident from the expressions in (37) and (38) that in a certain core given by $\xi > 1/\alpha_1$ i.e. outside the boundary layer region, fluid flows in both the primary and the secondary flow directions with uniform velocity. The primary flow moves with the velocity which is equal to the velocity of the moving plate and is unaffected by rotation and magnetic field. The primary and secondary induced magnetic fields h_x and h_y vary linearly with η and are considerably affected by rotation and magnetic field.

Case III: $M^2 \gg 1$ and $K^2 \sim O(1)$

In this case also boundary layer type flow is expected. For boundary layer flow near the upper plate *η = 1*, we obtain the velocity and induced magnetic field from the equations (23) to (25) as

$$u = e^{-\alpha_2 \xi}\left[\cos\beta_2\xi - \frac{2K^2}{M^2}\sin\beta_2\xi\right], \tag{39}$$

$$v = \frac{2K^2}{M^2} - e^{-\alpha_2 \xi}\left[\sin\beta_2\xi + \frac{2K^2}{M^2}\cos\beta_2\xi\right], \tag{40}$$

$$h_x = \frac{1}{M}\left[1 - e^{-\alpha_2 \xi}\left\{\cos\beta_2\xi - \frac{3K^2}{M^2}\sin\beta_2\xi\right\}\right], \tag{41}$$

$$h_y = \frac{2K^2\xi}{M^2} + \frac{1}{M}\left[-\frac{3K^2}{M^2} + e^{-\alpha_2 \xi}\left\{\sin\beta_2\xi + \frac{3K^2}{M^2}\cos\beta_2\xi\right\}\right], \tag{42}$$

where $\alpha_2 = M$ and $\beta_2 = \dfrac{K^2}{M}$. (43)

The expressions (39) to (43) demonstrate the existence of a thin Hartmann boundary layer of thickness $O(1/\alpha_2)$ adjacent to moving plate of the channel. The thickness of this boundary layer decreases with increase in M. Similar type of boundary layer appears near lower plate of the channel. Outside the boundary layer region, fluid velocity and induced magnetic field become

$$u \approx 0, \quad v \approx \frac{2K^2}{M^2}, \tag{44}$$

$$h_x \approx \frac{1}{M}, \qquad h_y \approx \frac{K^2}{M^2}\left(2\xi - \frac{3}{M}\right). \tag{45}$$

The expressions in (44) and (45) show that, in a certain core given by $\xi > 1/\alpha_2$ i.e. outside the boundary layer region, the fluid flows in secondary flow direction only with uniform velocity and has considerable effects of rotation and magnetic field. The primary induced magnetic field h_x is uniform and is unaffected by rotation while the secondary induced magnetic field h_y is affected by both the rotation and magnetic field and varies linearly with η.

4 Heat Transfer Characteristics

We shall now discuss heat transfer characteristics of the steady hydromagnetic Couette flow of a viscous incompressible electrically conducting fluid in a rotating system when the upper and lower plates of the channel are maintained at uniform temperatures T_1 and T_0 respectively, where $T_0 < T < T_1$, T being fluid temperature.

The energy equation taking viscous and Joule dissipations into account is given by

$$0 = \alpha^* \frac{d^2T}{dz^2} + \frac{\upsilon}{C_p}\left[\left(\frac{du^*}{dz}\right)^2 + \left(\frac{dv^*}{dz}\right)^2\right] + \frac{1}{\sigma\rho C_p}\left[\left(\frac{dH_x^*}{dz}\right)^2 + \left(\frac{dH_y^*}{dz}\right)^2\right], \tag{46}$$

where α^* and C_p are thermal diffusivity and specific heat at constant pressure respectively.

Boundary conditions for temperature field are

$$T = T_0 \text{ at } z = 0 \text{ and } T = T_1 \text{ at } z = L. \tag{47}$$

Making use of the non-dimensional variables defined in equation (16), equation (46), in non-dimensional form, becomes

$$\frac{d^2\theta}{d\eta^2} + E_r P_r\left[\left\{\left(\frac{du}{d\eta}\right)^2 + \left(\frac{dv}{d\eta}\right)^2\right\} + M^2\left\{\left(\frac{dh_x}{d\eta}\right)^2 + \left(\frac{dh_y}{d\eta}\right)^2\right\}\right] = 0, \tag{48}$$

where $\theta = \dfrac{T - T_0}{T_1 - T_0}$, $E_r = \dfrac{U_0}{C_p(T_1 - T_0)}$ and $P_r = \dfrac{\upsilon}{\alpha^*}$. θ , E_r and P_r are non-dimensional fluid temperature, Prandtl number and Eckert number respectively.

Boundary conditions (47), in non-dimensional form, become

$$\theta(0) = 0 \text{ and } \theta(1) = 1. \tag{49}$$

The analytical solution of fluid velocity and induced magnetic field from (23) to (25) are used in equation (48), and the resulting differential equation subject to the boundary conditions (49) is solved numerically with the help of MATLAB software. The numerical values of the rate of heat transfer at the lower and upper plates are also computed with the help of MATLAB software from the energy equation (48).

5 Results and Discussion

To study the effects of magnetic field and rotation on the flow field the numerical values of both the primary and secondary fluid velocities and primary and secondary induced magnetic fields, computed from analytical solution (23) to (25) reported in section 2 by MATLAB software, are displayed graphically versus channel width variable η in Figures 1 to 4 for various values of magnetic parameter M^2 and rotation parameter K^2. It is evident from Figure 1 that primary velocity *u* decreases whereas secondary velocity *v* increases on increasing M^2 which implies that magnetic field has retarding influence on the primary flow whereas it has reverse influence on the secondary flow. It is revealed from Figure 2 that primary velocity *u* and secondary velocity *v* increases on increasing K^2 which implies that rotation tends to accelerate fluid flow in both the primary and secondary flow directions.

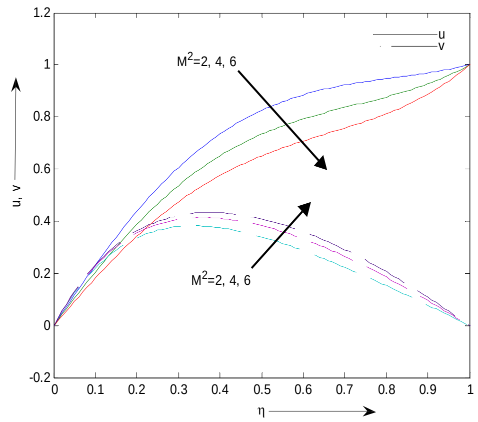

Figure 1: Velocity profiles when $K^2 = 7$

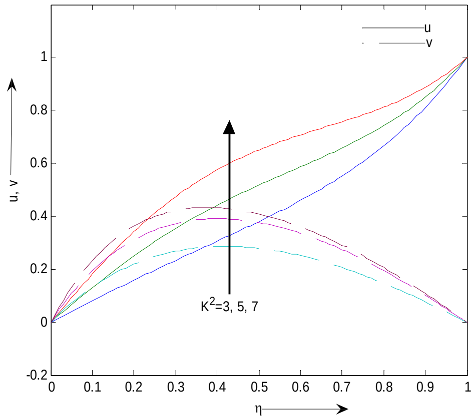

Figure 2: Velocity profiles when $M^2 = 6$

It is noticed from Figure 3 that primary induced magnetic field h_x decreases whereas secondary induced magnetic field h_y increases on increasing M^2 which implies that magnetic field has tendency to reduce primary induced magnetic field whereas it has reverse effect on the secondary induced magnetic field. Figure 4 reveals that both the primary induced magnetic field h_x and secondary induced magnetic field h_y increase on increasing K^2 which implies that rotation tends to enhance both the primary and secondary induced magnetic fields

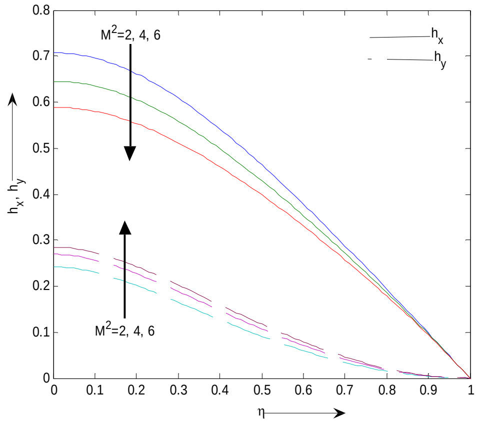

Figure 3: Magnetic field profiles when $K^2 = 7$

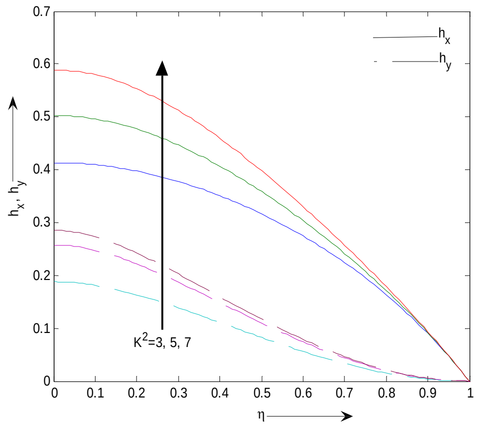

Figure 4: Magnetic field profiles when $M^2 = 6$

To study the effects of magnetic field and rotation on fluid temperature, the numerical solution of energy equation, computed with the help of MATLAB software, is presented graphically versus channel width variable η in Figures 5 to 8 for various values of M^2, K^2, Prandtl number P_r and Eckert number E_r. It is evident from Figure 5 that fluid temperature θ decreases in the region near the lower plate whereas it increases in the region $0.25 < \eta \le 1$ on increasing M^2 which implies that magnetic field tends to reduce fluid temperature in the region near lower plate of the channel whereas it has reverse effect on the fluid temperature in most of the region of the channel (i.e. $0.25 < \eta \le 1$). It is noticed from Figure 6 that, with the increase in K^2, fluid temperature θ increases in the region $0 \le \eta < 0.85$ where as it decreases in the region near upper plate of the channel which implies that rotation tends to enhance fluid temperature in most of the region of the channel (i.e. $0 \le \eta < 0.85$) whereas it has reverse effect on fluid temperature in the region near upper plate of the channel.

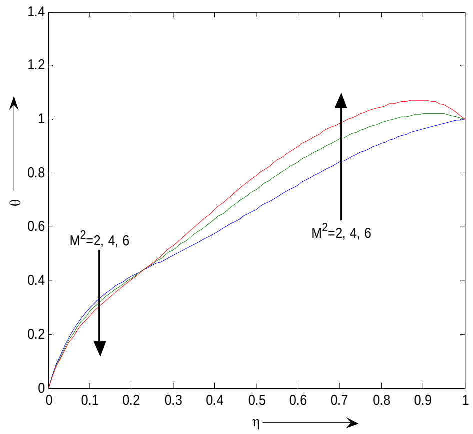

Figure 5: Fluid temperature profiles when $K^2 = 7$, $P_r = 0.71$ and $E_r = 0.8$

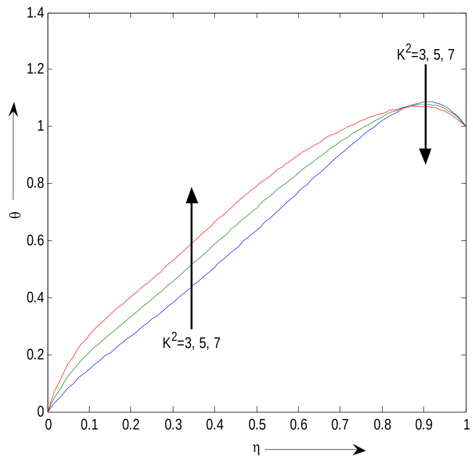

Figure 6: Fluid temperature profiles when $M^2 = 6$, $P_r = 0.71$ and $E_r = 0.8$

It is revealed from the Figure 7 that fluid temperature θ decreases on decreasing Prandtl number P_r. Since P_r is a measure of the strength of viscosity and thermal conductivity of fluid. P_r decreases when thermal conductivity of fluid increases. Therefore, we conclude from above result that thermal diffusion tends to reduce fluid temperature throughout the channel. It may be noted that variation in fluid temperature θ along the channel width is linear for liquid metal i.e. mercury ($P_r = 0.03$) whereas it is non-linear for air and water. It is observed from

Figure 8 that fluid temperature θ increases on increasing E_r which implies that viscous dissipation has tendency to increase fluid temperature throughout the channel.

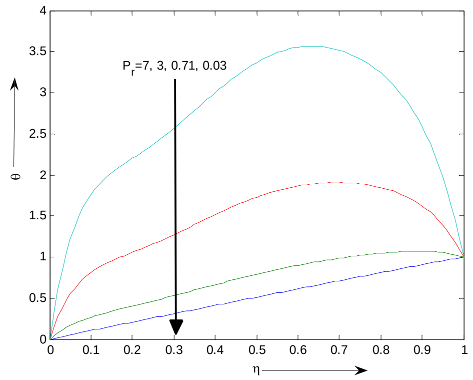

Figure 7: Fluid temperature profiles when $M^2 = 6,\ K^2 = 7$ and $E_r = 0.8$

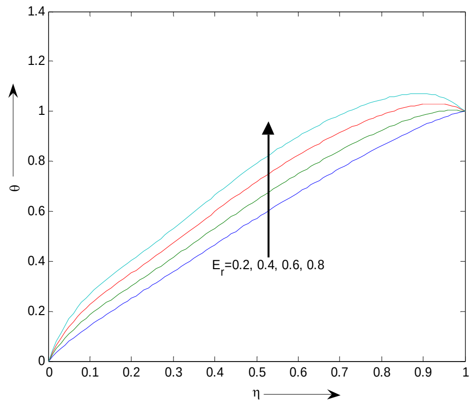

Figure 8: Fluid temperature profiles when $M^2 = 6,\ K^2 = 7$ and $P_r = 0.71$

The numerical values of the primary shear stress τ_x and secondary shear stress τ_y at the lower and upper plates, computed from the analytical expression (26) mentioned in section 2 by MATLAB software, are displayed in tabular form in tables 1 and 2 while that of primary mass flow rate Q_x and secondary mass flow rate Q_y, computed from analytical expression (27) mentioned in section (2) by MATLAB software, are presented in tabular form in table 3 for various values of M^2 and K^2. It is revealed from table 1 that primary shear stress at the lower plate i.e. $\tau_x\big|_{\eta=0}$ decreases whereas secondary shear stress at the lower plate i.e. $\tau_y\big|_{\eta=0}$ behaves in oscillatory manner on increasing M^2 which implies that magnetic field tends to reduce primary shear stress at the lower plate. It is observed from table 1 that both $\tau_x\big|_{\eta=0}$ and $\tau_y\big|_{\eta=0}$ increase on increasing K^2 which implies that rotation has tendency to enhance both the primary and secondary shear stress at the lower plate. It is noticed from table 2 that primary shear stress at the upper plate i.e. $\tau_x\big|_{\eta=1}$ increases on increasing M^2 whereas it decreases on increasing K^2 which implies that magnetic field tends to enhance primary shear stress at the upper plate whereas rotation has reverse effect on it. It is found from table 2 that, with an increase in M^2, secondary shear stress at the upper plate i.e. $\tau_y\big|_{\eta=1}$ increases when $K^2 = 5$ and 7 and it increases, attains a maximum, and then decreases when $K^2 = 3$. On increasing K^2, $\tau_y\big|_{\eta=1}$ increases, attains a maximum, and then decreases when $M^2 = 2$ and 4 and it increases when $M^2 = 6$. This implies that when the effects of magnetic field and rotation are significant, magnetic field and rotation tend to enhance secondary shear stress at the upper plate. It is evident from table 3 that primary mass flow rate Q_x decreases on increasing M^2 whereas it increases on increasing K^2 which implies that magnetic field tends to reduce primary mass flow rate whereas rotation has reverse effect on it. It is noticed from table 3 that secondary mass flow rate Q_y decreases when $K^2 = 3$ whereas it increases when $K^2 = 5$ and 7 on increasing M^2 and Q_y increases an increasing K^2 which implies that rotation tends to enhance secondary mass flow rate where as magnetic field tends to enhance secondary mass flow rate when $K^2 \geq 5$.

Table 1: Primary and secondary shear stress at the lower plate

$M^2 \rightarrow$ / $K^2 \downarrow$	$\tau_x\|_{\eta=0}$			$\tau_y\|_{\eta=0}$		
	2	4	6	2	4	6
3	1.2597	1.0055	0.8142	1.6875	1.6592	1.6085
5	1.8450	1.5626	1.3272	2.3779	2.4075	2.3914
7	2.3618	2.0975	1.8560	2.8348	2.9177	2.9492

Table 2: Primary and secondary shear stress at the upper plate

$M^2 \rightarrow$ / $K^2 \downarrow$	$\tau_x\|_{\eta=1}$			$-\tau_y\|_{\eta=1}$		
	2	4	6	2	4	6
3	1.1484	1.6955	2.1646	0.7612	0.7853	0.7809
5	0.7073	1.2657	1.7645	0.8664	0.9781	1.0349
7	0.3901	0.9085	1.3945	0.7809	0.9689	1.0946

Table 3: Primary and secondary mass flow rates

$M^2 \rightarrow$ / $K^2 \downarrow$	Q_x			Q_y		
	2	4	6	2	4	6
3	0.5271	0.4633	0.4134	0.1943	0.1939	0.1883
5	0.6277	0.5600	0.5027	0.2393	0.2537	0.2579
7	0.7072	0.6454	0.5889	0.2419	0.2693	0.2853

The numerical values of rate heat transfer at the lower and upper plates are computed with the help of MATLAB software and are displayed in the tabular form in tables 4 and 5 for various values of M^2, K^2, P_r, and E_r. It is evident from table 4 that rate of heat transfer at the lower plate i.e. $\frac{d\theta}{d\eta}\Big|_{\eta=0}$ decreases on increasing M^2 and it increases on increasing K^2. With an increase in M^2, the rate of heat transfer at the upper plate i.e. $\frac{d\theta}{d\eta}\Big|_{\eta=1}$ increases when $K^2 = 3$ and it decreases, attains a minimum and then increases when $K^2 = 5$ and 7. $\frac{d\theta}{d\eta}\Big|_{\eta=1}$ decreases, attains a minimum, and then increases in magnitude on increasing K^2 when $M^2 = 2$ while it decreases on increasing K^2 when $M^2 = 4$ and 6. Thus we conclude that magnetic field tends to reduce rate of heat transfer at the lower plate whereas rotation has reverse effect on it. Magnetic field tends to enhance rate of heat transfer at the upper plate and rotation has reverse effect on it when $M^2 \geq 4$. It may be noted that there exists reverse flow of heat near upper plate on increasing K^2 when $M^2 = 2$ and also reverse flow of heat takes place near upper plate on increasing M^2 when $K^2 = 5$ and 7.

Table 4: Rate for heat transfer at the lower and upper plates when $P_r = 0.71$ and $E_r = 0.8$

$M^2 \rightarrow$ / $K^2 \downarrow$	$\left(\frac{d\theta}{d\eta}\right)_{\eta=0}$			$-\left(\frac{d\theta}{d\eta}\right)_{\eta=1}$		
	2	4	6	2	4	6
3	2.2594	2.0690	1.9231	0.1071	1.1276	2.2078
5	3.5726	3.3396	3.1245	-0.0768	0.8627	1.8924
7	4.8665	4.6671	4.4485	-0.2156	0.6370	1.5965

Table 5: Rate for heat transfer at the lower and upper plates when $M^2 = 6$ and $K^2 = 7$

$E_r \rightarrow$ / $P_r \downarrow$	$\left(\frac{d\theta}{d\eta}\right)_{\eta=0}$				$-\left(\frac{d\theta}{d\eta}\right)_{\eta=1}$			
	0.2	0.4	0.6	0.8	0.2	0.4	0.6	0.8
0.01	1.0121	1.0243	1.0364	1.0486	-0.9909	-0.9817	-0.9726	-0.9634
0.03	1.0364	1.0729	1.1093	1.1457	-0.9726	-0.9451	-0.9177	-0.8903
0.71	1.8621	2.7242	3.5863	4.4485	-0.3509	0.2983	0.9474	1.5965
3.0	4.6427	8.2855	11.9282	15.5710	1.7428	4.4856	7.2285	9.9713
7.0	9.4997	17.9995	26.4992	34.9989	5.3999	11.7998	18.1998	24.5997

It is noticed from table 5 that $\frac{d\theta}{d\eta}\Big|_{\eta=0}$ decreases on decreasing P_r and it increases on increasing E_r. $\frac{d\theta}{d\eta}\Big|_{\eta=1}$ decreases, attains a minimum, and then increases in magnitude on decreasing P_r. $\frac{d\theta}{d\eta}\Big|_{\eta=1}$ decreases in magnitude on increasing E_r when $P_r \leq 0.03$, it decreases, attains a minimum and then increases on increasing E_r when $P_r = 0.71$ and increases on increasing E_r when $P_r \geq 3$. Thus we conclude that thermal diffusion tends to reduce rate of heat transfer at the lower plate whereas viscous dissipation has reverse effect on it. Thermal diffusion tends to reduce rate of heat transfer at the upper plate when $P_r \geq 3$ whereas it has reverse effect on the rate of heat transfer at the upper plate when $P_r \leq 0.03$. Viscous dissipation tends to enhance rate of heat transfer at the upper plate when $P_r \geq 3$ whereas it has reverse effect on the rate of heat transfer at the upper plate when $P_r \leq 0.03$. It may be noted that there exists reverse flow of heat near upper plate on decreasing P_r and also there exists reverse flow of heat near upper plate on increasing E_r when $P_r = 0.71$.

6 Conclusion

Present investigation deals with the theoretical study of steady MHD Couette flow of class-II in a rotating system. The significant results are summarized below:

(i) Magnetic field has retarding influence on the primary flow and it has reverse influence on the secondary flow.

(ii) Rotation tends to accelerate fluid flow in both the primary and secondary flow directions.

(iii) Magnetic field has tendency to reduce primary induced magnetic field whereas it has reverse effect on the secondary induced magnetic field.

(iv) Rotation tends to enhance both the primary and secondary induced magnetic fields.

(v) Magnetic field tends to reduce fluid temperature in the region near lower plate of the channel whereas it has reverse effect on fluid temperature in most of the region of the channel (i.e. $0.25 < \eta \leq 1$).

(vi) Rotation tends to enhance fluid temperature in most of the region of the channel (i.e. $0 \leq \eta < 0.85$) whereas it has reverse effect on fluid temperature in the region near upper plate of the channel.

(vii) Thermal diffusion tends to reduce fluid temperature throughout the channel whereas viscous dissipation has reverse effect on it.

(viii) Magnetic field tends to reduce primary shear stress at the lower plate. Rotation has tendency to enhance both the primary and secondary shear stress at the lower plate.

(ix) Magnetic field tends to enhance primary shear stress at the upper plate whereas rotation has reverse effect on it. When the effects of magnetic field and rotation are significant, magnetic field and rotation tend to enhance secondary shear stress at the upper plate.

(x) Magnetic field tends to reduce primary mass flow rate whereas rotation has reverse effect on it. Rotation tends to enhance secondary mass flow rate whereas magnetic field tends to enhance secondary mass flow rate when $K^2 \geq 5$.

(xi) Magnetic field tends to enhance rate of heat transfer at the upper plate and rotation has reverse effect on it when $M^2 \geq 4$. There exists reverse flow of heat on increasing K^2 when $M^2 = 2$ and also reverse flow of heat takes place on increasing M^2 when $K^2 = 5$ and *7*.

(xii) Thermal diffusion tends to reduce rate of heat transfer at the lower plate whereas viscous dissipation has reverse effect on it. Thermal diffusion tends to reduce rate of heat transfer at the upper plate when $P_r \geq 3$ whereas it has reverse effect on the rate of heat transfer at the upper plate when $P_r \leq 0.03$. Viscous dissipation tends to enhance rate of heat transfer at the upper plate when $P_r \geq 3$ whereas it has reverse effect on the rate of heat transfer at the upper plate when $P_r \leq 0.03$. There exists reverse flow of heat near upper plate on decreasing P_r and also there exists reverse flow of heat near upper plate on increasing E_r when $P_r = 0.71$.

ACKNOWLEDGEMENT

Authors are grateful to referees for their valuable suggestions and also thankful to UGC, New Delhi (INDIA) for providing financial assistance.

References

[1] H. Yamasaki, S. Kabashima, S. Shioda and Y. Okuno, Unsteady discharge and fluid flow in a closed-cycle disk MHD generator, *AIAA Journal of Propulsion and Power*, **4**, (1988), 61-67.

[2] V. I. Kabakov and Y. I. Yantovsky, Solar pond magnetohydrodynamic generator for hydrogen production, *Int. J. Hydrogen Energy*, **18**, (1993), 19-23.

[3] C. Vogin and A. Alemany, Analysis of the flow in a thermo-acoustic MHD generator with conducting walls, *Eur. J. Mechanics-B/Fluids*, **26**, (2007), 479-493.

[4] S. O. Macheret, M. N. Shneider and R. B. Miles, Magnetohydrodynamic and electrohydrodynamic control of hypersonic flows of weakly ionized plasmas, *AIAA J.*, **42**, (2004), 1378-1387.

[5] J. Zueco, O. A. Beg, H. S. Takhar and V. R. Prasad, Thermophoretic hydromagnetic dissipative heat and mass transfer with lateral mass flux, heat

source, Ohmic heating and thermal conductivity effects: network simulation numerical study, *Applied Thermal Engineering*, **29**, (2009), 2808-2815.

[6] O. A. Beg, A. Y. Bakier, V. R. Prasad and S. K. Ghosh, Non-similar, laminar, steady, electrically-conducting forced conviction liquid metal boundary layer flow with induced magnetic field effects, *Int. J. Thermal Sciences*, **48** (8), (2009), 1596-1606.

[7] R. N. Jana, N. Datta and B. S. Mazumder, Magnetohydrodynamic Couette flow and heat transfer in a rotating system, *J. Phys. Soc. Japan*, **42**, (1977), 1034-1039.

[8] R. N. Jana and N. Datta, Hall effects on MHD Couette flow in a rotating system, *Czech. J. Phys.*, **B30**, (1980), 659-667.

[9] G. S. Seth and M. K. Maiti, MHD Couette flow and heat transfer in a rotating system, *Ind. J. Pure and Appl. Math.*, **13**, (1982), 931-945.

[10] G. Mandal, K. K. Mandal and G. Choudhury, On combined effects of Coriolis force and Hall current on steady MHD Couette flow and heat transfer, *J. Phys. Soc. Japan*, **51**, (1982), 2010-2015.

[11] G. Mandal and K. K. Mandal, Effects of Hall current on MHD Couette flow between thick arbitrarily conducting plates in a rotaing system, *J. Phys. Soc. Japan*, **52**, (1983), 470-477.

[12] G. S. Seth and N. Ahmad, Effects of Hall current on MHD Couette flow and heat transfer in a rotating system, *J. ISTAM*, **30**, (1985), 177-188.

[13] A. Kumar, G. S. Seth and A. Talib, Hydromagnetic Couette flow in a rotating system with Hall effects, *Acta Ciencia Indica*, **33 M**, (2007), 937-945.

[14] G. S. Seth, R. N. Jana and M. K. Maiti, Unsteady hydromagnetic Couette flow in a rotating system, *Int. J. Engng. Sci.*, **20**, (1982), 989-999.

[15] G. S. Seth, R. Nandkeolyar, N. Mahto and S. K. Singh, MHD Couette flow in a rotating system in the presence of inclined magnetic field, *Appl. Math. Sci.*, **3** (59), (2009), 2919-2932.

[16] G. S. Seth, Md. S. Ansari and R. Nandkeolyar, Unsteady hydromagnetic Couette flow within porous plates in a rotating system, *Adv. Appl. Math. Mech.*, **2** (3), (2010), 286-302.

[17] G. S. Seth, Md. S. Ansari and R. Nandkeolyar, Unsteady hydromagnetic Couette flow induced due to accelerated movement of one of the porous plates of the channel in a rotating system, *Int. J. Appl. Math. Mech.*, **6** (7), (2010), 24-42.

[18] G. S. Seth, Md. S. Ansari and R. Nandkeolyar, Effects of rotation and magnetic field on unsteady Couette flow in a porous channel, *J. Appl. Fluid Mech.*, **4** (2), (2011), (To appear).

[19] G. S. Seth, R. Nandkeolyar and Md. S. Ansari, Hall effects on oscillatory hydromagnetic Couette flow in a rotating system, *Int. J. Acad. Res.*, **1** (2), (2009), 6-17.

[20] P. Chandran, N. C. Sacheti and A. K. Singh, Effects of rotation on unsteady hydromagnetic Couette flow, *J. Astrophys. Space Sci*, **202**, (1993), 1-10.

[21] A. K. Singh, N. C. Sacheti and P. Chandran, Transient effects on Magnetohydrodynamic Couette flow with rotation, *Int, J. Engng. Sci.*, **32**, (1994), 133-139.

[22] K. D. Singh, An oscillatory hydromagnetic Couette flow in a rotating system, *ZAMM*, **80**, (2000), 429-432.

[23] T. Hayat, S. Nadeem and S. Asghar, Hydromagnetic Couette flow of a Oldroyd-B fluid in a rotating system, *Int. J. Engng. Sci.*, **42**, (2004), 65-78.

[24] T. Hayat, S. Nadeem, A. M. Siddiqui and S. Asghar, An oscillatory hydromagnetic non-Newtonian flow in a rotating system, *Appl. Math. Lett.*, **17**, (2004), 609-614.

[25] M. Guria, S. Das, R. N. Jana and S. K. Ghosh, Oscillatory Couette flow in the presence of inclined magnetic field, *Meccanica*, **44**, (2009), 555-564.